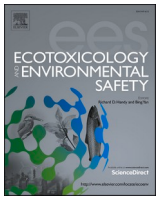
Ecotoxicology and Environmental Safety 303 (2025) 118799



Contents lists available at ScienceDirect

Ecotoxicology and Environmental Safety

journal homepage: www.elsevier.com/locate/ecoenv



Integrative *in silico* and *in vitro* approach for clarifying mode of action to activate estrogen receptor alpha and lipid accumulation by methiocarb

Da-Hyun Jeong [a], Rajesh Kumar Pathak [b], Eunhee Lee [a], Jun-Mo Kim [c,*], Hee-Seok Lee [a,d,**]

[a] GreenTech-based Food Safety Research Group, BK21 Four, Department of Food Science and Biotechnology, Chung-Ang University, 4726 Seodong-daero, Anseong-si, Gyeonggi-do 17546, Republic of Korea
[b] Pere Virgili Institute for Health Research (IISPV), Tarragona 43005, Spain
[c] Department of Animal Science and Technology, Chung-Ang University, 4726 Seodong-daero, Anseong-si, Gyeonggi-do 17546, Republic of Korea
[d] Department of Food Safety and Regulatory Science, Chung-Ang University, 4726 Seodong-daero, Anseong-si, Gyeonggi-do 17546, Republic of Korea

ARTICLE INFO

Edited by Tao Zhang

Keywords:
Methiocarb
Estrogen receptor alpha
Binding affinity
Agonist
Lipid accumulation

ABSTRACT

Disruption of estrogen receptor alpha (ERα) by endocrine-active pesticides may contribute to lipid metabolic dysregulation. We aimed to clarify the docking dynamics of methiocarb with ERα and evaluate its potential to induce lipid accumulation through ERα activation using non-animal testing systems. Molecular docking predicted favorable binding between methiocarb and ERα, primarily through interactions involving the amino group. This prediction was validated using ERα reporter gene assays. Methiocarb-induced lipid accumulation was assessed in 3T3-L1 adipocytes, with or without co-treatment using the ERα antagonist methyl-piperidino-pyrazole (MPP). Methiocarb significantly activated ERα transcriptional activity and promoted ERα-dependent lipid accumulation. Co-treatment with MPP attenuated this effect, whereas antagonists for the glucocorticoid receptor (RU-486) and ERβ (PHTPP) had no effect. Methiocarb increased the expression of adipogenic and lipogenic transcription factors, including PPARγ, C/EBPα, FAS, and SREBP1, as well as the adipocyte-specific marker FABP4, in an ERα-dependent manner. Methiocarb binding to ERα promotes lipid accumulation and upregulates adipogenic/lipogenic transcriptional networks. This approach highlights the utility of ERα-mediated screening to identify potential metabolic disruptors among structurally related pesticides.

1. Introduction

Because of their rapid decomposition and relatively low toxicity to mammals compared with that of organochlorine and organophosphate pesticides (Dias et al., 2015; Rahman et al., 2017), carbamates affecting the activity of enzymes containing acetylcholinesterase (AChE) in exposed pests (Blažková et al., 2009) have been applied worldwide as insecticides. Several critical effects of carbamate insecticides due to AChE inhibition have been reported (Zhang and Lee, 2006). Carbamates inhibit AChE, an enzyme that catalyzes the hydrolysis of the neurotransmitter acetylcholine (ACh). This increases ACh at neuronal synapses or neuromuscular junctions, resulting in increased stimulation of nerve endings (Jokanović, 2009).

Methiocarb ($C_{11}H_{15}NO_2S$), a carbamate insecticide, has been widely used as an acaricide, molluscicide, and bird repellent in food, natural water, and soil since the 1960s (United States Environmental Protection Agency (EPA) (EPA), 1994; Altinok et al., 2006; European Union, 2018; Lentola et al., 2021). Therefore, various routes have exposed food materials and the environment to methiocarb. Llasera and Bernal-González (Bernal-González, 2001) reported that the level of methiocarb contamination in a groundwater sample was 5.4 μg/L. The residual range of methiocarb in surface river water was 7–117 ng/L (Fytianos et al., 2007). The average levels of methiocarb were 20.73 μg/kg in oranges, 18.82 μg/kg in dates and plums, and 7.46 μg/kg in tangerines (Blasco et al., 2005). Additionally, average concentrations of methiocarb in wine and soil samples were 0.84 and 0.02 μg/kg, respectively (Gonzalez et al., 2022).

It is considered a hazardous pesticide in various countries, and

* Corresponding author.
** Corresponding author at: GreenTech-based Food Safety Research Group, BK21 Four, Department of Food Science and Biotechnology, Chung-Ang University, 4726 Seodong-daero, Anseong-si, Gyeonggi-do 17546, Republic of Korea
E-mail addresses: junmokim@cau.ac.kr (J.-M. Kim), hslee0515@cau.ac.kr (H.-S. Lee).

https://doi.org/10.1016/j.ecoenv.2025.118799
Received 26 May 2025; Received in revised form 25 July 2025; Accepted 30 July 2025
Available online 2 August 2025
0147-6513/© 2025 The Authors. Published by Elsevier Inc. This is an open access article under the CC BY license (http://creativecommons.org/licenses/by/4.0/).

maximum residue levels have been established based on data concerning the critical effects of methiocarb and its metabolites. Recently, the endocrine-disrupting potential of methiocarb was reported (Gea et al., 2022). Methiocarb did not disrupt estrogen biosynthesis; however, it exhibited estrogenic effects in an *in vitro* transactivation assay (TA).

Endocrine-disrupting chemicals (EDCs) primarily interfere with natural hormones because of their strong ability to bind to estrogen receptors (ER) (Tabb and Blumberg, 2006). Estrogen signaling is altered via genomic and non-genomic pathways by interacting directly with receptors. The genomic pathway involves gene transcription and is initiated by the binding of EDCs to the cytosol and/or nuclear ER. In contrast, the non-genomic pathway is induced by membrane-bound ER with ligands and involves signaling proteins (Kiyama et al., 2014). The Organization for Economic Cooperation and Development (OECD) has established international standard testing methods to determine the EDCs, and the ERα specific TA assay using hERα-HeLa 9903 cell line was adopted as PBTG No. 455 (OECD, 2021). The estrogen-ER complex of the ER membrane also modulates the activity of other types of biomarkers (O'Lone et al., 2004). The membrane ER response promotes transcriptional activation, resulting in a dimeric interaction between nuclear and extranuclear mechanisms that regulates vascular function, cell growth, and lipid accumulation (Grün and Blumberg, 2006; Meyer et al., 2009).

Based on the above, we considered that the estrogenic effect of methiocarb may be caused by lipid accumulation in the ERα pathway. Furthermore, previous studies have reported an association between exposure to estrogenic substances and obesity (Grün and Blumberg, 2006). Therefore, we conducted a hybrid *in silico/in vitro* approach to test our hypothesis. The molecular dynamics simulations and subsequent analyses were investigated using computational models, followed by experimental studies. We confirmed the ERα-specific agonistic effect of methiocarb using the hERα-HeLa 9903 ER TA assay (OECD, 2021). Adipocyte formation induced by methiocarb in the presence and absence of the ERα selective antagonist, i.e., methyl-piperidino-pyrazole (MPP), was determined to clarify the relationship between lipid accumulation and ERα activation in 3T3-L1 cells.

2. Materials and methods

2.1. Computational analysis of the interaction between ERα and methiocarb

2.1.1. Preparations

The 3D structures of BPA and methiocarb were downloaded from the PubChem database. The co-crystallized E2 was obtained from the ERα structure. LigPrep module of Schrödinger Maestro was used for ligand preparation by adding hydrogen atoms, optimizing bond lengths and angles, and identifying the lowest-energy conformer. Chirality, tautomeric states, stereochemistry, and ring conformations were also accurately assigned. (Schrödinger Release 2023–4; Schrödinger, LLC, New York, NY, USA) (Schrödinger, 2025). The ERα 3D structure (PDB ID: 1ERE) was downloaded from the Protein Data Bank. The structure was prepared using Schrödinger Maestro's Protein Preparation Wizard. This automated process removed solvent molecules, incorporated hydrogen atoms, completed missing loop regions, capped terminal ends, optimized protonation states, and corrected erroneous hydrogen bonding. Finally, the prepared protein structure underwent energy minimization employing the OPLS4 force field. Default parameters were applied in the Glide receptor grid generation module, including a van der Waals radius scaling factor of 1.0 and a partial charge cutoff of 0.25. A receptor grid was ultimately generated by selecting the centroid of the workspace ligand for the molecular docking studies.

2.2. Molecular docking and binding energy calculations using molecular mechanics/generalized born and surface area continuum solvation (MM/GBSA)

Molecular docking of E2, BPA, and methiocarb with ERα was conducted using the standard precision protocol of Glide with default settings (Friesner et al., 2004). The binding energy (ΔG_{bind}) of docked complexes was calculated using the Prime MM/GBSA module in Schrödinger. The calculations employed the Volume Surface Generalized Born (VSGB) solvation model and the OPLS4 force field (Lu et al., 2021).

2.2.1. Density function theory (DFT) analysis

DFT was applied to evaluate the chemical reactivity of E2, BPA, and methiocarb by determining its frontier molecular orbitals, including the highest occupied molecular orbital (HOMO) and the lowest unoccupied molecular orbital (LUMO) (https://doi.org/10.1021/acsomega.4c08626). All calculations were performed using the Jaguar module in Schrödinger Maestro with standard settings (Schrödinger, 2025).

2.2.2. Molecular dynamics simulation (MDS)

We conducted MDS of ERα, ERα–E2, ERα–BPA, and ERα–methiocarb docked complexes using Desmond (Schrödinger, 2025) to evaluate the dynamic behavior of ERα before and after ligand binding, as described in Method S1 of the Supporting Information.

2.2.3. Post-MDS MM/GBSA binding energy calculations

Binding energy calculations using molecular dynamic simulation trajectories were conducted using the MM/GBSA method with thermal_mmgbsa.py python script provided by Schrödinger Maestro (Schrödinger, 2025). The calculated energy components included van der Waals interactions, Coulombic forces, hydrogen bonding, lipophilic interactions, π–π stacking, generalized Born electrostatic solvation energy, and total ΔG_{bind}(Yazdani et al., 2023).

2.3. ERα-mediated disruption of lipid metabolism by methiocarb in the experimental study

2.3.1. Reporter gene assays

Reporter gene assays were performed following the OECD TG No. 455 using the ERα-HeLa-9903 cell line (JCRB, Osaka, Japan) to evaluate the ERα agonistic activity of methiocarb. To assess the androgen receptor (AR) antagonistic activity of methiocarb, luciferase reporter gene assays were conducted using the 22Rv1/MMTV_GR-KO cell line according to OECD TG No. 458 (OECD, 2023), as described in Method S2 of the Supporting Information.

2.3.2. Differentiation, oil red O, and DAPI staining

Differentiation of 3T3-L1 adipocytes (ATCC, Rockville, MD, USA) was induced after pre-incubation for 24 h. The detailed protocol for 3T3-L1 adipocyte differentiation and staining has been described in our previous publications (Kim et al., 2021).

2.3.3. Expression of adipogenic/lipogenic mRNAs using methiocarb

Total RNAs extracted from differentiated adipocytes were analyzed after transcription to cDNA coupled with primers. Our previous publication described mRNA expression detection details (Ahmed and Atlas, 2016).

2.3.4. Expression of adipogenic/lipogenic proteins using methiocarb

Cellular proteins of differentiated adipocytes were analyzed using western blotting. The transferred proteins were then allowed to react sequentially with primary and secondary antibodies, as previously described (Kim et al., 2021).

2.4. Statistical analysis

All statistical analyses were performed using GraphPad Prism version 8 (GraphPad Software, San Diego, CA, USA). One-way analysis of variance (ANOVA) was used to evaluate differences between groups, followed by Dunnett's post hoc test to compare each treatment group to the vehicle control (0.1 % dimethyl sulfoxide, DMSO). Results are expressed as mean ± standard deviation (SD) (n = 3). Statistical significance was considered at $p < 0.05$ (*), $p < 0.01$ (**), and $p < 0.001$ (***).

3. Results

3.1. Molecular docking and MM/GBSA quantification of the binding energies with ERα

The docking score for methiocarb was −5.139 kcal/mol. However, the docking score of control compounds E2 and BPA was predicted as −10.392 and −7.964 kcal/mol. To further evaluate the binding interaction, MM/GBSA binding free energy calculations were performed on the docked complexes. The predicted binding free energy for methiocarb was −31.28 kcal/mol. These results suggest that methiocarb exhibits a favorable binding affinity for ERα. The binding energies and key interacting amino acid residues are illustrated in Fig. 1 and summarized in Table S1 of the Supporting Information.

3.2. DFT calculations

The HOMO and LUMO of the methiocarb were calculated using DFT. This analysis was performed through the Jaguar module in Schrödinger, offering insights into the energy of these orbitals. Fig. 2 presents the HOMO and LUMO visualizations of the methiocarb. According to Fig. 2, the calculated energy gap induced by methiocarb varied by 5.59 eV. This suggested that methiocarb have similar values like E2 and BPA, exhibited significant stability and reactivity, enabling interactions with ERα. The visualized molecular orbitals are depicted in Fig. 2 and calculated energy values are summarized in Table S2 of the Supporting Information.

3.3. MDS

MD simulations were employed to explore the dynamic properties of ERα in its unbound form and when complexed with methiocarb. Key simulation parameters were assessed to examine the stability and dynamic behavior of ERα. Root mean square deviation (RMSD) analyses of the simulation trajectories provided insights into structural stability, with lower RMSD values indicating higher stability. These simulations were conducted over a 500 ns period to observe structural deviations over time. The RMSD of ERα indicated an average of 2.24 Å, while that of the ERα complex with E2, BPA and methiocarb was 2.02, 2.10 and 2.57 Å, respectively (Fig. 3). The findings indicated that methiocarb reached equilibrium and formed stable complexes like a control compound E2 and BPA. However, fluctuations were observed in the ERα–methiocarb complex after 100 ns. Around 350 ns, the RMSD trend appeared to stabilize, indicating that the system reached a relatively stable conformation. The root mean square fluctuation (RMSF) analysis was also performed to assess the flexibility of amino acid residues within ERα and its ligand-bound states over 500 ns. The average RMSF for unbound ERα was 1.16 Å, while that for the ERα complex with E2, BPA and methiocarb was 0.97, 0.95 and 1.15 Å, respectively.

The interaction between ERα E2, BPA and methiocarb was monitored throughout the simulation. This interaction can be categorized into hydrogen bonds, hydrophobic interactions, ionic interactions, and water bridges. In our analysis, E2 interacts with Glu353, Leu387, Phe404 and His524. Glu353, Phe404 and His524 also interact with BPA. However, amino groups on the methiocarb structure mainly interacted with ERα residues Leu387 (Fig. 4).

3.4. Post-MDS binding energy calculations using MM/GBSA

This comprehensive analysis provided a detailed assessment of binding affinity. We derived the ΔG_{bind} value, as detailed in Table 1, using post-MD MM/GBSA calculations. The predicted average binding energy of methiocarb with ERα was −48.69 kcal/mol. However, the average binding energy for E2 and BPA was predicted as −62.60 and −53.74 kcal/mol. These computational predictions collectively indicated that methiocarb can interact with ERα in ways that may impact its normal functions.

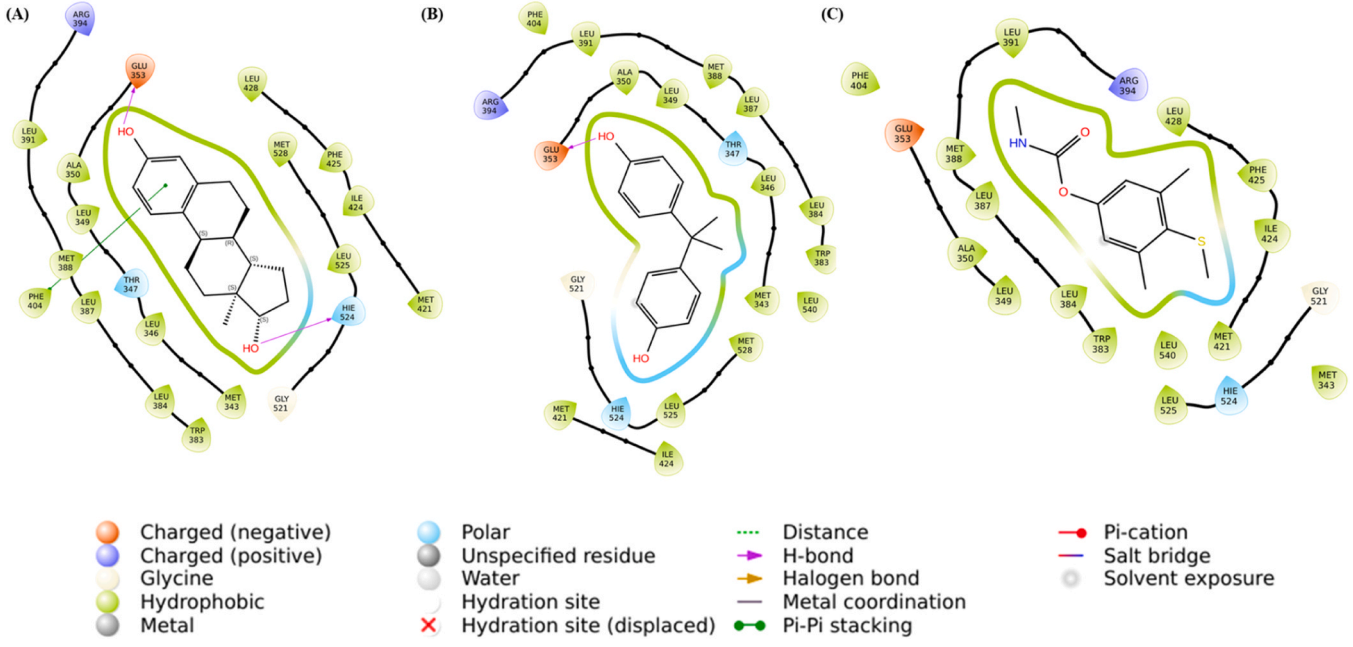


Fig. 1. Two-dimensional interaction diagrams showing the binding of (A) E2, (B) BPA, and (C) methiocarb to estrogen receptor alpha (ERα).

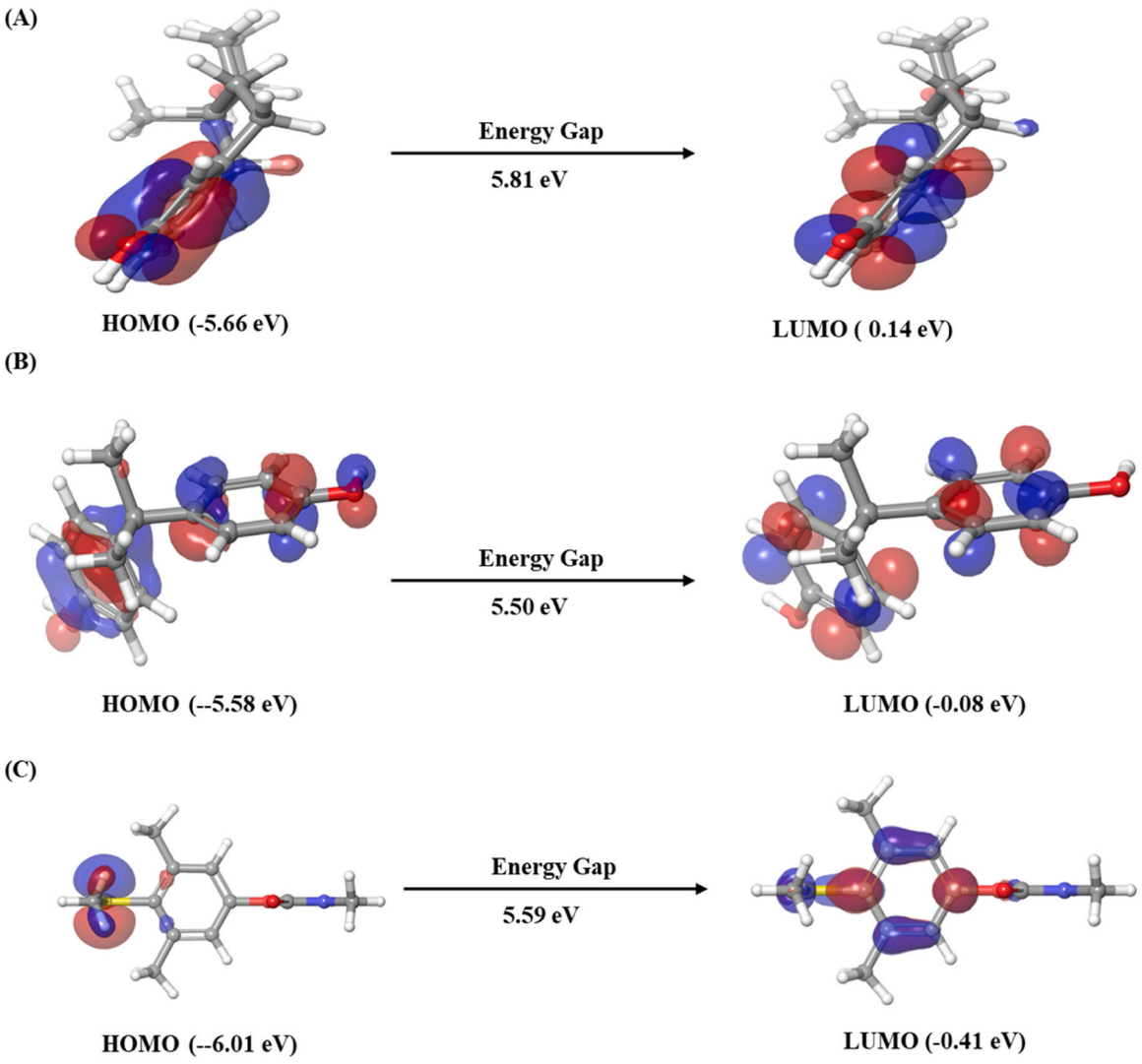


Fig. 2. Frontier molecular orbital analysis of (A) E2, (B) BPA and (C) methiocarb using density functional theory (DFT), showing the highest occupied molecular orbital (HOMO) and lowest unoccupied molecular orbital (LUMO).

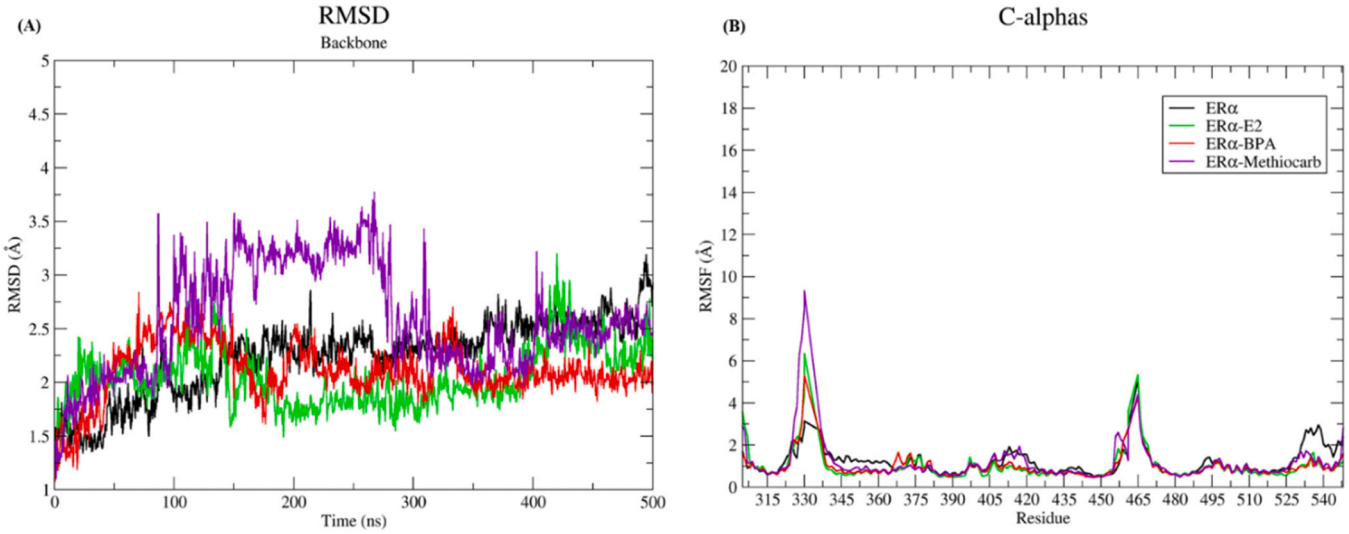


Fig. 3. Molecular dynamics simulation of estrogen receptor alpha (ERα) over 500 ns. (A) Root-mean-square deviation (RMSD) of the ERα backbone shows structural equilibration followed by stabilization. (B) Root-mean-square fluctuation (RMSF) of ligand-binding domain residues, indicating residue-level flexibility.

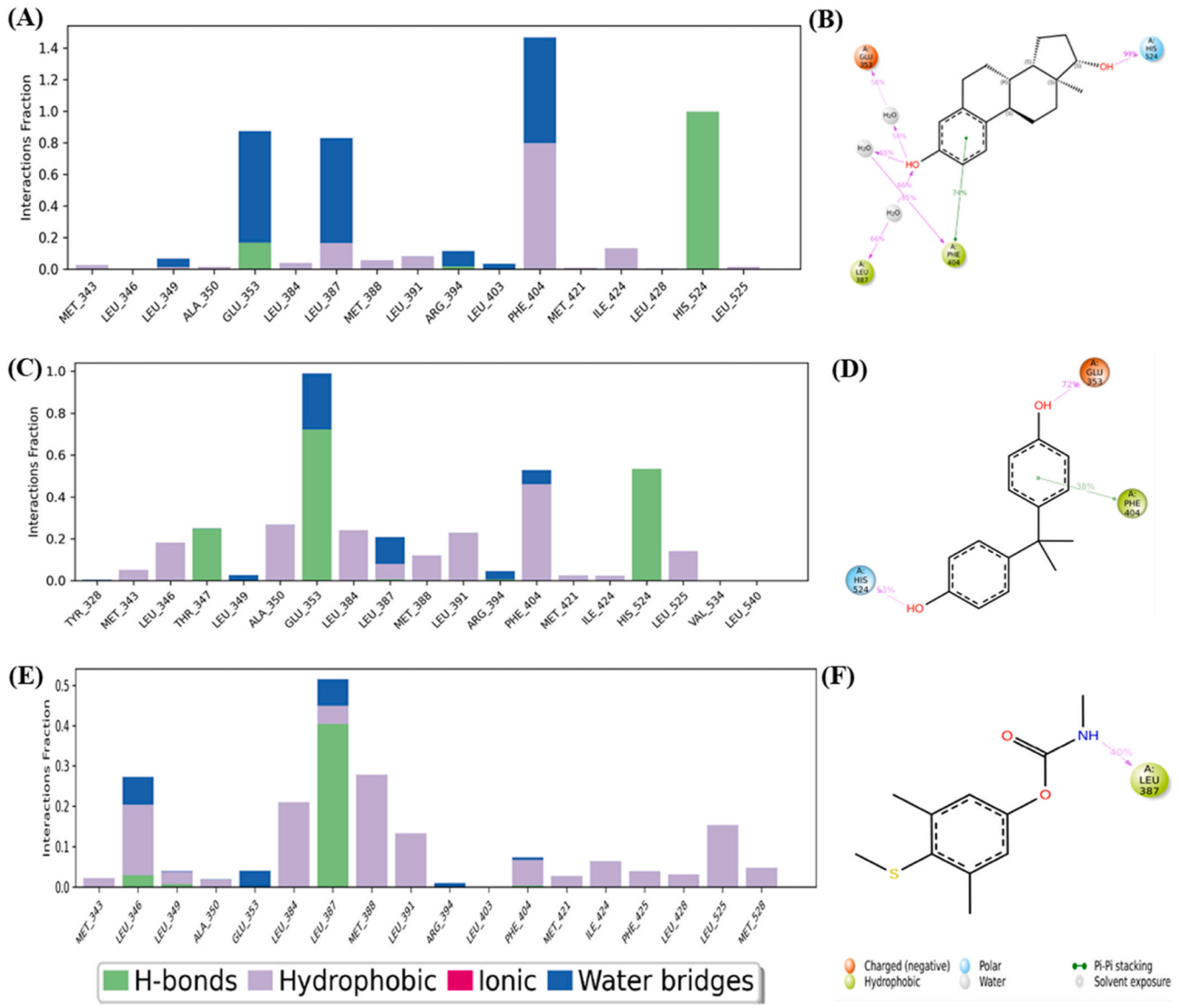


Fig. 4. E2, BPA and methiocarb binding interaction analysis to estrogen receptor alpha (ERα) through molecular dynamics simulations. (A) Timeline of protein–ligand contacts over 500 ns. (B) Percentage occurrence of ligand interactions with ERα residues during the simulation. Only interactions present for more than 30 % of the simulation time are shown.

Table 1
Predicted average binding free energies (kcal/mol) for estradiol (E2), bisphenol A (BPA), and methiocarb with ERα, calculated using MM/GBSA based on molecular dynamics simulation trajectories.

Compound	ΔG_{vdw}	ΔG_{coul}	ΔG_{Hbond}	ΔG_{Lipo}	ΔG_{Pack}	ΔG_{SolGB}	ΔG_{bind}
E2	−43.96	−9.64	−0.80	−27.74	−0.54	18.73	−62.60
BPA	−35.72	−15.29	−1.18	−23.30	−0.52	21.06	−53.74
Methiocarb	−39.84	−5.64	−0.00	−16.63	−0.03	12.89	−48.69

ΔG_{vdw}: Contribution of van der Waals interaction energy to binding free energy; **ΔG_{coul}:** Contribution of Coulomb energy to binding free energy; **ΔG_{Hbond}:** H-bonding contributions to binding free energy; **ΔG_{Lipo}:** Lipophilic energy contribution to binding free energy; **ΔG_{Pack}:** π-π packing energy contribution to binding free energy; **ΔG_{SolGB}:** Generalized Born electrostatic solvation energy contribution to binding free energy. **ΔG_{bind}:** Total binding free energy.

3.5. ER-agonistic effect induced by methiocarb

The predicted ERα affinity induced by methiocarb was validated through *in vitro* ERα transcriptional activation assays. Methiocarb was classified as an ERα agonist with a PC_{10} (Log M) value of −5.15 ± 0.18 (Table 2 and Fig. 5). These results indicated that methiocarb may cause the lipid accumulation associated with ERα.

3.6. Lipid accumulation induced by methiocarb

Oil red O staining was conducted to investigate methiocarb-dependent lipid accumulation alongside the positive control, −5 log M

Table 2
Agonistic effects of methiocarb on estrogen receptor alpha (ERα).

Assays		Quantitative activity values (Log M)	
ERα agonist	Chemicals	PC_{10}	PC_{50}
	E2 (17β-estradiol)	−11.69 ± 0.03	−10.67 ± 0.04
	Methiocarb	−5.15 ± 0.18	-

The values are provided as the mean ± SD.

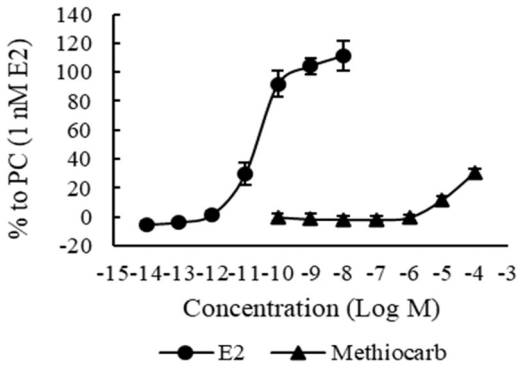


Fig. 5. Dose–response curve of estrogen receptor alpha (ERα) transcriptional activation induced by methiocarb.

bisphenol A (BPA), well-known as an ERα agonistic endocrine-disrupting chemical. The results of the cell-viability assay indicated that methiocarb showed intrinsic toxicity against 3T3-L1 adipocytes at −4 log M (data not shown). Based on these cytotoxicities, methiocarb was added up to −5 log M to confirm lipid-accumulation induction. Lipid droplet accumulation was significantly promoted by 1.3- and 1.5-fold after treatment with −5 and −6 log M, respectively (Fig. 6).

3.7. Confirmation of ERα-dependent lipid accumulation induced by methiocarb

The effect of methiocarb on lipid accumulation was assessed in the presence and absence of an ERα selective antagonist, MPP, to elucidate the regulatory role of ERα. At 10 μM methiocarb, lipid accumulation was significantly suppressed by 23.7 % in the presence of 5 μM MPP (Fig. 7). These results indicated that methiocarb induced lipid accumulation in an ERα-dependent manner.

3.8. Expression of adipogenic/lipogenic mRNAs

The respective expression levels of PPARγ and C/EBPα were increased by methiocarb at 10 μM and inhibited by MPP at 5 μM (Fig. 8). The expression levels of lipogenic mRNAs (FAS and SREBP1) and the adipocyte-specific factor FABP4 were enhanced by methiocarb. In addition, methiocarb significantly increased the expression of adipocyte-specific factor FABP4. In contrast, the mRNA expression levels of FAS, SREBP, and FABP4 decreased in the presence of MPP (Fig. 8).

3.9. Expression of adipogenic/lipogenic proteins

The expression levels of proteins related to adipogenesis and lipogenesis were quantitatively measured to elucidate the mechanism underlying methiocarb-mediated lipid accumulation (Fig. 9). Methiocarb (10 μM) significantly increased the expression levels of PPARγ and C/EBPα, and their respective expression levels were inhibited by MPP of 5 μM, an ERα-selective antagonist. The expression levels of lipogenic proteins (FAS and SREBP1) were also significantly increased by methiocarb treatment. Conversely, co-treatment with MPP inhibited their methiocarb-induced expression level. Additionally, the quantitative expression of the FABP4 was significantly increased by methiocarb. The decrease in the expression level of FABP4 after co-treatment with MPP was also significant compared with that in the methiocarb treatment group.

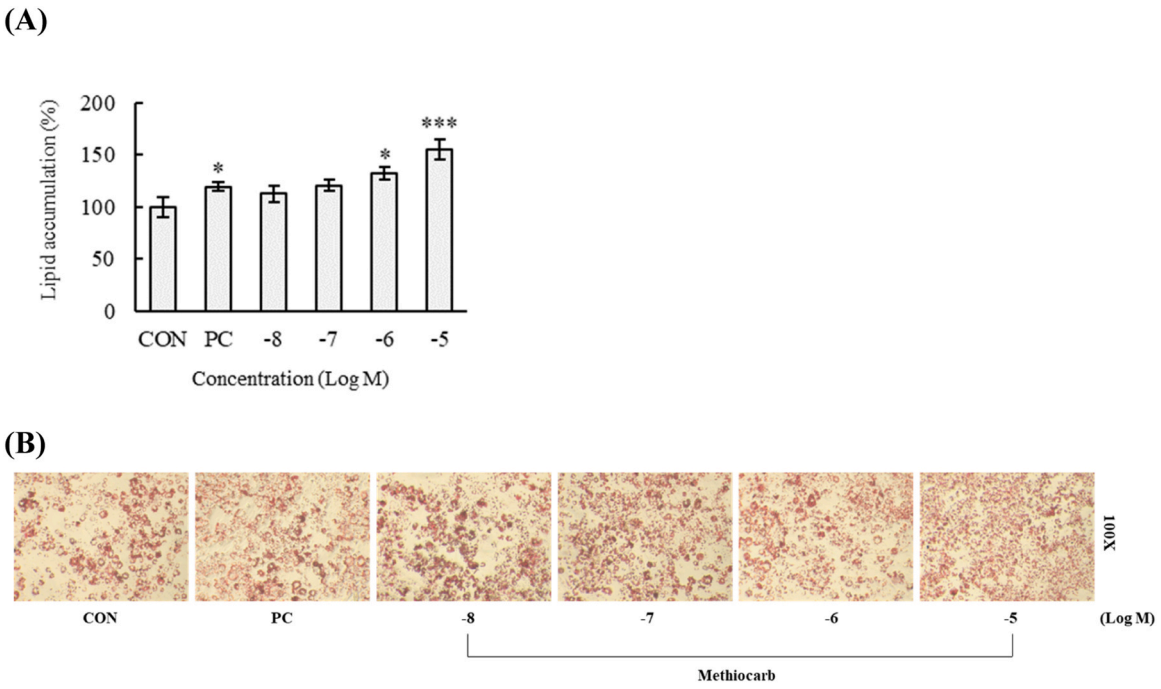


Fig. 6. (A) Lipid accumulation induced by methiocarb in 3T3-L1 adipocytes. (B) Oil Red O staining image at 100 × magnification. $p < 0.05$ (*), $p < 0.01$ (**), and $p < 0.001$ (***); analyzed by one-way ANOVA followed by Dunnett's test.

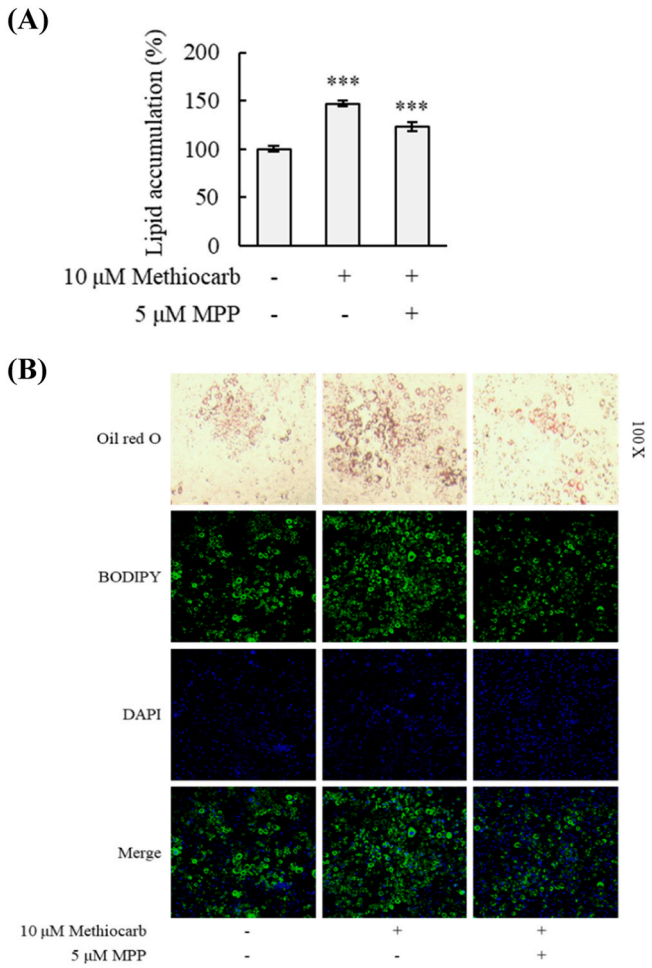


Fig. 7. (A) Lipid accumulation induced by methiocarb with or without methyl-piperidino-pyrazole (MPP), an estrogen receptor alpha (ERα) selective antagonist. (B) BODIPY and Oil Red O staining images at 100 × magnification. $p < 0.05$ (*), $p < 0.01$ (**), and $p < 0.001$ (***); analyzed by one-way ANOVA followed by Dunnett's test.

4. Discussion

In this study, we tested the hypothesis that methiocarb-induced ERα disruption may cause lipid accumulation. Methiocarb was classified as an ERα agonist using the international standard ER TA and the ERα-HeLa-9903 cell line, which was adopted by the OECD. Furthermore, methiocarb enhanced the ERα-dependent accumulation of lipid droplets by regulating adipogenic/lipogenic differentiation. To our knowledge, this is the first report on the association between the methiocarb-mediated endocrine-disrupting effect and lipid accumulation.

Several studies have identified that the ERα-agonistic effect via binding affinity to ERα provides key evidence for the potential development of an ERα-dependent lipid accumulation mechanism. The well-known mediated EDCs BPA and bisphenol S have been reported to significantly induce cellular lipid accumulation (Ahmed and Atlas, 2016; Lee and Park, 2019). The ER-agonistic pesticides quizalofop-p-ethyl and 1, 3, 5-Tris(4-hydroxyphenyl)-4-propyl-1H-pyrazole induce ER-dependent adipogenesis through proliferation of adipose-derived stem cells (Zhang et al., 2016; Biserni et al., 2019). Additionally, the critical effects of four ERα-agonistic organophosphorus pesticides that induced lipid accumulation were blocked in the presence of MPP, a selective ERα antagonist (Kim et al., 2021). Also, as expected, the activation of ERα by methiocarb was able to induce ERα-dependent lipid accumulation in adipocytes. In contrast, methiocarb did not increase the GR-mediated glucocorticoid response element luciferase activity. The results in the adipocytes indicated that methiocarb-dependent lipid accumulation did not change significantly in the presence of GR antagonist, RU486 (Fig. 7 A). Regarding the interference by ERβ on methiocarb-induced lipid accumulation in adipocytes, the results indicated that an ERβ selective antagonist, PHTPP (4-[2-Phenyl-5,7-bis(trifluoromethyl)pyrazolo[1,5-*a*]-pyrimidin-3-yl] phenol) treatment alone did not induce significant lipid accumulation, and PHTPP co-treatment led to no significant changes in the level of methiocarb-induced lipid accumulation (Fig. 10 A). In terms of the relationship between activation of AR and adipocyte differentiation, Blouin et al. (2009) reported that androgen levels have been linked to inhibition of adipogenesis, and inactivating androgens are found in differentiated adipocytes. In the present study, DHT-induced androgen response element luciferase activity was inhibited in the presence of methiocarb as expected (Fig. 10B). The AR antagonistic effect of methiocarb could potentially result in fat accumulation *in vivo*.

Although BPA exhibited stronger ERα agonistic activity than methiocarb, its adipogenic effect in 3T3-L1 cells was notably weaker. This apparent discrepancy highlights the mechanistic complexity of adipogenesis, which is not determined solely by the degree of ERα activation. It is important to note that the ER transcriptional activation assay primarily reflects genomic signaling pathways. In contrast, adipocyte differentiation and lipid accumulation are also influenced by non-genomic ER signaling (e.g., ERK/MAPK, p38/MAPK, PI3K/AKT, PLC/PKC) and other receptor-mediated mechanisms, such as those involving GR or AR (Marino et al., 2006; Levin, 2011). Therefore, a direct quantitative comparison between transcriptional activation and lipid accumulation may have inherent limitations.

Methiocarb, despite being a partial ERα agonist with lower binding affinity compared to BPA, induced greater lipid accumulation. This may involve the activation of various endocrine pathways, encompassing both genomic and non-genomic ER signaling, as well as other adipogenic and lipogenic regulators such as C/EBPα, and potential synergistic interactions among these pathways. In contrast, BPA-induced lipid accumulation was significantly reduced by co-treatment with the ERα antagonist MPP, indicating a more direct ERα-dependent mechanism (see Figure S1). While the current study focused on elucidating ERα-mediated effects of methiocarb, further investigation is warranted to clarify the contribution of non-ER pathways to its adipogenic potential.

Structurally, we propose that the amino-substituted phenyl ring in methiocarb contributes binding to ERα with docking score of −5.139 kcal/mol based on docking results. For comparison, E2, the endogenous ERα ligand, yields docking scores between −8.1 and −12.0 kcal/mol depending on receptor conformation and software used (Zhang et al., 2020; Hutton, 2022; Bake et al., 2025). While methiocarb exhibits lower affinity to ERα than E2, the interaction involves key hydrogen-bonding residues, suggesting that methiocarb may function as a partial ERα agonist. This is supported by its ability to activate transcriptional responses and induce downstream lipid accumulation. Prior studies have also identified that the phenyl ring in a compound's structure enhances its ERα docking capacity (Stauffer et al., 2000; Li et al., 2010). Thus, we anticipate that the amino group of methiocarb selectively promotes ERα binding and activates lipid-accumulating pathways. While our approach does not include animal experimentation, the combination of *in silico* molecular modeling and *in vitro* cell-based assays provides a robust and ethical alternative for mechanistic evaluation. This integrated method can serve as a predictive framework for identifying receptor-mediated endocrine-disrupting effects of environmental chemicals, particularly where *in vivo* studies are impractical or ethically restricted.

Although the concentrations used in this study exceed typical environmental levels, they were selected based on toxicological principles to identify receptor-level mechanistic effects and establish points of departure (POD) for future risk assessment. In vitro studies investigating endocrine-disrupting chemicals often apply higher concentrations to

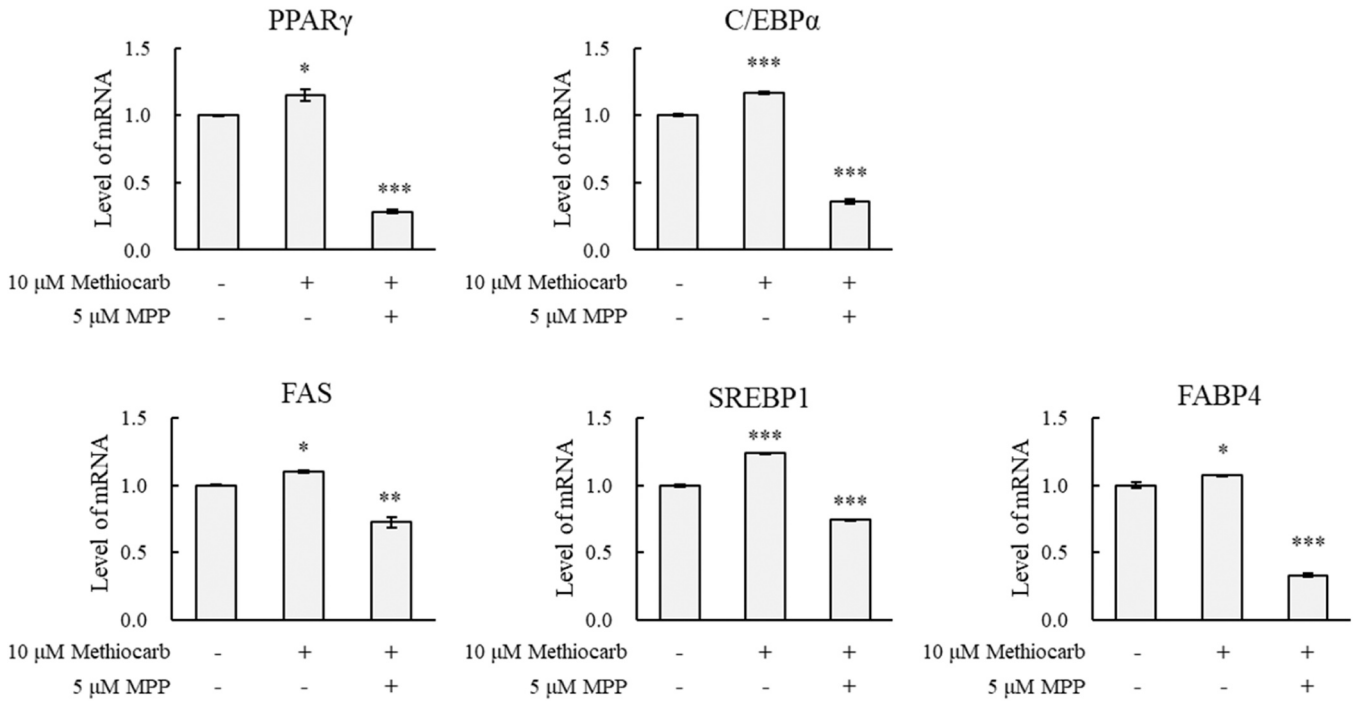


Fig. 8. Expression of adipogenic (PPARγ and C/EBPα), lipogenic (FAS and SREBP1), and adipocyte marker (FABP4) mRNAs induced by methiocarb with or without methyl-piperidino-pyrazole (MPP). $p < 0.05$ (*), $p < 0.01$ (**), and $p < 0.001$ (***); analyzed by one-way ANOVA followed by Dunnett's test.

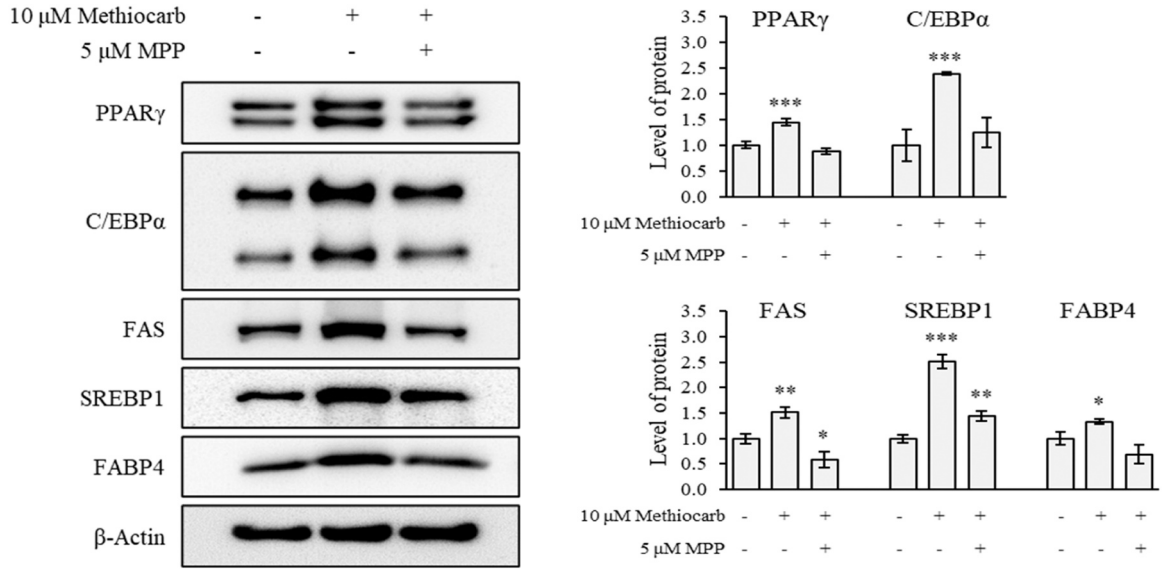


Fig. 9. Detection of adipogenic proteins (PPARγ and C/EBPα), lipogenic proteins (FAS and SREBP1), and FABP4 protein induced by methiocarb in the presence and absence of MPP. $p < 0.05$ (*), $p < 0.01$ (**), and $p < 0.001$ (***); analyzed by one-way ANOVA followed by Dunnett's test.

uncover biological activity. Moreover, given that EDCs frequently exhibit non-monotonic dose–response (NMDR) characteristics, it is important to evaluate their effects across a broad range of concentrations, as emphasized by previous studies (Vandenberg et al., 2012; Gore et al., 2015). Importantly, the frequency and persistence of environmental exposure, rather than concentration alone, may play a more critical role in long-term biological outcomes. Therefore, the aim of the current study is not to issue a direct environmental alarm, but to provide mechanistic insights that will inform follow-up in vivo studies, which are currently in the design phase.

As described in the Introduction, methiocarb is managed by establishing an acceptable daily intake (ADI). The ADI value of methiocarb was determined to be 0.02 mg/kg bw in 1998 (FAO, 1999). Additionally, the scientific panels of the EFSA adopted an updated ADI value of 0.00025 mg/kg body weight per day based on the relevant POD value (EFSA, 2018). In terms of endocrine-disrupting properties, EFSA scientific panels agree that methiocarb should not be considered a reproductive hazardous pesticide and is not defined as an endocrine disruptor (EFSA, 2018). Interpreting the data from the *in vitro* model used, we present novel scientific evidence that methiocarb and its hepatic metabolites were characterized as ERα agonizts using the international standard test method (OECD, 2021). Our results indicate that methiocarb induces ERα-mediated lipid accumulation by upregulating adipogenic and lipogenic transcription factors. Although these findings are

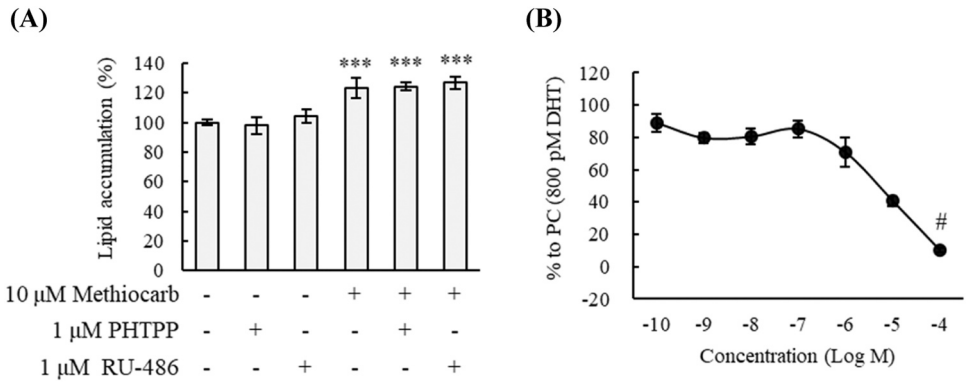


Fig. 10. (A) Effect of glucocorticoid receptor (GR) antagonist RU-486 and estrogen receptor beta (ERβ) antagonist PHTPP on methiocarb-induced lipid accumulation. (B) Inhibition of dihydrotestosterone (DHT)-induced androgen response element luciferase activity by methiocarb. The cytotoxic concentration of the test chemical is indicated by a hashtag (#). $p < 0.05$ (*), $p < 0.01$ (**), and $p < 0.001$ (***); analyzed by one-way ANOVA followed by Dunnett's test.

derived from cell-based models, several studies have emphasized the validity of such models in elucidating receptor-mediated endocrine effects. In contrast, the POD values used in regulatory toxicology, which are predominantly based on animal studies and adopted by organizations such as FAO and EFSA, may have limitations in capturing mechanistic disruptions at the molecular level. Therefore, bridging these mechanistic insights with traditional regulatory endpoints remains a critical need in risk assessment. Additionally, recent advances in computational toxicology particularly AI-driven virtual screening and multi-scale modeling enable rapid identification of potential endocrine disruptors, enhancing environmental health risk assessment (https://doi.org/10.3389/ftox.2022.981928; https://doi.org/10.1186/s12909-024–06163-x). These approaches strengthen in silico predictive capabilities for prioritizing high-risk compounds requiring experimental validation and regulatory scrutiny.

Lastly, our findings demonstrate the potential of integrated in silico–in vitro methods as a feasible and ethical tool for screening endocrine-disrupting chemicals. This strategy aligns with current efforts to reduce reliance on animal testing while ensuring mechanistic clarity in chemical risk assessment.

5. Conclusions

The ERα agonistic effects of methiocarb were determined in computational analysis and OECD PBTG No.455 ER TA assay using the ERα-HeLa-9903 cell line. Furthermore, we found, for the first time, that the activation of ERα by methiocarb promoted lipid accumulation by upregulating adipogenic/lipogenic transcription factors in 3T3-L1 adipocytes. These novel findings provide crucial scientific evidence for identifying the relationship between ERα-mediated endocrine-disrupting carbamate insecticides having a similar structure to that of methiocarb exposure, particularly in the context of obesity development.

Ethics statement

Not applicable. No human participants or live animal experiments were involved in this study.

Funding

This study was supported by a grant from the National Research Foundation of Korea (NRF), funded by the Korean government (MSIT) [RS-2024–00345893]. Additional support was provided by the Ministry of Food and Drug Safety of Korea [grant number 21162MFDS078]. This research was also supported by the Chung-Ang University Graduate Research Scholarship (Academic Scholarship for College of Biotechnology and Natural Resources) in 2023.

CRediT authorship contribution statement

Da-Hyun Jeong: Investigation, Writing – original draft, Writing – review & editing. **Rajesh Kumar Pathak:** Validation, Writing – original draft. **Eunhee Lee:** Validation, Writing – review & editing. **Jun-Mo Kim:** Conceptualization, Data curation. **Hee-Seok Lee:** Conceptualization, Data curation, Funding acquisition, Project administration, Investigation, Validation, Writing – original draft, Writing – review & editing.

Declaration of Competing Interest

The authors declare that they have no known competing financial interests or personal relationships that could have appeared to influence the work reported in this paper.

Appendix A. Supporting information

Supplementary data associated with this article can be found in the online version at doi:10.1016/j.ecoenv.2025.118799.

Data availability

No data was used for the research described in the article.

References

Ahmed, S., Atlas, E., 2016. Bisphenol S- and bisphenol A-induced adipogenesis of murine preadipocytes occurs through direct peroxisome proliferator-activated receptor gamma activation. Int. J. Obes. 40, 1566–1573. https://doi.org/10.1038/ijo.2016.95.

Altinok, I., Capkin, E., Karahan, S., Boran, M., 2006. Effects of water quality and fish size on toxicity of methiocarb, a carbamate pesticide, to rainbow trout. Environ. Toxicol. Pharmacol. 22, 20–26. https://doi.org/10.1016/j.etap.2005.11.002.

Bake, M.M., Fofack, H.M.T., Abdelli, W., Ntie-Kang, F., 2025. Unlocking potential natural products from African sources targeting overexpressed estrogen receptor alpha (ERα) in breast cancer: in silico studies. Comput. Biol. Med. 164, 107521. https://doi.org/10.1016/j.compbiomed.2024.107521.

Bernal-González, Llasera M.P.G., 2001. M. Presence of carbamate pesticides in environmental waters from the northwest of Mexico: determination by liquid chromatography. Water Res. 35, 1933–1940. https://doi.org/10.1016/S0043-1354(00)00478-4.

Biserni, M., Mesnage, R., Ferro, R., et al., 2019. Quizalofop-p-ethyl induces adipogenesis in 3T3-L1 adipocyte. Toxicol. Sci. 170, 452–461. https://doi.org/10.1093/toxsci/kfz097.

Blasco, C., Font, L.G., Manes, J., Pico, Y., 2005. Screening and evaluation of fruit samples for four pesticide residues. J. AOAC Int. 88, 847–854. https://doi.org/10.1093/jaoac/88.3.847.

Blažková, M., Mičková-Holubová, B., Rauch, P., Fukal, L., 2009. Immunochromatographic colloidal carbon-based assay for detection of methiocarb in surface water. Biosens. Bioelectron. 25, 753–758. https://doi.org/10.1016/j.bios.2009.08.023.

Blouin, K., Nadeau, M., Mailloux, J., et al., 2009. Pathways of adipose tissue androgen metabolism in women: depot differences and modulation by adipogenesis. Am. J. Physiol. Endocrinol. Metab. 296, E244–E255. https://doi.org/10.1152/ajpendo.00039.2008.

Dias, E., Costa, F.G., Morais, S., de Lourdes Pereira, M., 2015. A review on the assessment of the potential adverse health impacts of carbamate pesticides. Top. Public Health 197–212. https://doi.org/10.5772/59613.

EFSA, 2018. Peer review of the pesticide risk assessment of the active substance methiocarb. EFSA J. 16 (1), 5429. https://doi.org/10.2903/j.efsa.2018.5429.

European Union. Commission Implementing Decision (EU) 2018/840. Off J Eur Union.2018;L141/9–L141/12.⟨https://eur-lex.europa.eu/legal-content/EN/TXT/PDF/?uri=CELEX:32018D0840&rid=7⟩.

FAO, 1999. Pesticide residues in food—1998. Report of the Joint FAO/WHO Meeting. Plant Production and Protection Paper No. 148. Rome: FAO.

Friesner, R.A., Banks, J.L., Murphy, R.B., et al., 2004. Glide: a new approach for rapid, accurate docking and scoring. 1. method and assessment of docking accuracy. J. Med. Chem. 47, 1739–1749. https://doi.org/10.1021/jm0306430.

Fytianos, K., Pitarakis, K., Bobola, E., 2007. Monitoring of N-methylcarbamate pesticides in the pinios river (central Greece) by HPLC. Int. J. Environ. Anal. Chem. 86, 131–145. https://doi.org/10.1080/03067310500248171.

Gea, M., Zhang, C., Tota, R., et al., 2022. Assessment of five pesticides as endocrine-disrupting chemicals: effects on estrogen receptors and aromatase. Int. J. Environ. Res. Public Health 19, 1959. https://doi.org/10.3390/ijerph19041959.

Gonzalez, P.A., Dans, E.P., Dacal, A.C.A., et al., 2022. Differences in the levels of sulphites and pesticide residues in soils and wines under organic and conventional production methods. J. Food Compost. Anal. 112, 104714. https://doi.org/10.1016/j.jfca.2022.104714.

Gore, A.C., Chappell, V.A., Fenton, S.E., et al., 2015. EDC-2: the endocrine Society's second scientific statement on Endocrine-Disrupting chemicals. Endocr. Rev. 36 (6), E1–E150. https://doi.org/10.1210/er.2015-1010.

Grün, F., Blumberg, B., 2006. Environmental obesogens: organotins and endocrine disruption via nuclear receptor signaling. Endocrinology 147, S50–S55. https://doi.org/10.1210/en.2005-1129.

Hutton, M.B., 2022. In Silico and Cell Studies on the Interaction of the Herbicide Glyphosate with Estrogen Receptors [Master's thesis]. University of Canterbury. https://doi.org/10.26021/12755.

Jokanović, M., 2009. Medical treatment of acute poisoning with organophosphorus and carbamate pesticides. Toxicol. Lett. 190, 107–115. https://doi.org/10.1016/j.toxlet.2009.07.025.

Kim, J.T., Lee, H.J., Lee, H.S., 2021. Organophosphorus pesticides exert estrogen receptor agonistic effect determined using organization for economic cooperation and development PBTG 455, and induce estrogen receptor-dependent adipogenesis of 3T3-L1 adipocytes. Environ. Pollut. 283, 117090. https://doi.org/10.1016/j.envpol.2021.117090.

Kiyama, R., Zhu, Y., Kawaguchi, K., et al., 2014. Estrogen-responsive genes for environmental studies. Environ. Technol. Innov. 1, 16–28. https://doi.org/10.1016/j.eti.2014.09.001.

Lee, H.S., Park, Y., 2019. Identification of metabolic pathways related to the bisphenol A-induced adipogenesis in differentiated murine adipocytes by using RNA-sequencing. Environ. Res. 171, 161–169. https://doi.org/10.1016/j.envres.2019.01.017.

Lentola, A., Giorio, C., Bogialli, S., et al., 2021. Methiocarb metabolites are systemically distributed throughout corn plants grown from coated seeds. Environ. Chem. Lett. 19, 1887–1892. https://doi.org/10.1007/s10311-020-01098-3.

Levin, E.R., 2011. Extranuclear steroid receptors: roles in modulation of cell functions. Mol. Endocrinol. 25 (3), 377–384. https://doi.org/10.1210/me.2010-0492.

Li, J., Ma, M., Wang, Z., 2010. In vitro profiling of endocrine disrupting effects of phenols. Toxicol. Vitr. 24, 201–204. https://doi.org/10.1016/j.tiv.2009.09.008.

Lu, C., Wu, C., Ghoreishi, D., et al., 2021. OPLS4: improving force field accuracy on challenging regimes of chemical space. J. Chem. Theory Comput. 17, 4291–4300. https://doi.org/10.1021/acs.jctc.1c00302.

Marino, M., Galluzzo, P., Ascenzi, P., 2006. Estrogen signaling multiple pathways to impact gene transcription. Curr. Genom. 7 (8), 497–508. https://doi.org/10.2174/138920206779315737.

Meyer, M.R., Haas, E., Prossnitz, E.R., Barton, M., 2009. Non-genomic regulation of vascular cell function and growth by estrogen. Mol. Cell Endocrinol. 308, 9–16. https://doi.org/10.1016/j.mce.2009.03.009.

O'Lone, R., Frith, M.C., Karlsson, E.K., Hansen, U., 2004. Genomic targets of nuclear estrogen receptors. Mol. Endocrinol. 18, 1859–1875. https://doi.org/10.1210/me.2003-0044.

, 2021OECD, 2021. Test No. 455: Performance-Based Test Guideline for Stably Transfected Transactivation In Vitro Assays to Detect Estrogen Receptor Agonists and Antagonists. doi:10.1787/9789264265295-en.

, 2023OECD, 2023. Test No. 458: stably transfected human androgen receptor transcriptional activation assay for detection of androgenic and antiandrogenic activity of chemicals. OECD Guidelines for the Testing of Chemicals. Section 4. doi:10.1787/8e4a2fa1-en.

Rahman, M.M., Abd El-Aty, A., Na, T.W., et al., 2017. Simultaneous quantification of methiocarb and its metabolites, methiocarb sulfoxide and methiocarb sulfone, in five food products of animal origin using tandem mass spectrometry. J. Chromatogr. B 1060, 387–394. https://doi.org/10.1016/j.jchromb.2017.06.025.

Schrödinger L.L.C. What are the default settings for receptor grid generation in Glide? Schrödinger Knowledge Base. Article ID: 1842. Published 2024. Accessed April 24, 2025. ⟨https://www.schrodinger.com/kb/1842⟩.

Stauffer, S.R., Coletta, C.J., Tedesco, R., et al., 2000. Pyrazole ligands: structure−affinity/activity relationships and estrogen receptor-α-selective agonists. J. Med. Chem. 43, 4934–4947. https://doi.org/10.1021/jm000170m.

Tabb, M.M., Blumberg, B., 2006. New modes of action for endocrine-disrupting chemicals. Mol. Endocrinol. 20, 475–482. https://doi.org/10.1210/me.2004-0513.

United States Environmental Protection Agency (EPA). Methiocarb. R.E.D. FACTS. 1994. ⟨https://www3.epa.gov/pesticides/chem_search/reg_actions/reregistration/fs_PC-100501_1-Feb-94.pdf⟩.

Vandenberg, L.N., Colborn, T., Hayes, T.B., et al., 2012. Hormones and endocrine-disrupting chemicals: low-dose effects and nonmonotonic dose responses. Endocr. Rev. 33 (3), 378–455. https://doi.org/10.1210/er.2011-1050.

Yazdani, B., Sirous, H., Brogi, S., Calderone, V., 2023. Structure-based high-throughput virtual screening and molecular dynamics simulation for the discovery of novel SARS-CoV-2 NSP3 Mac1 domain inhibitors. Viruses 15 (12), 2291. https://doi.org/10.3390/v15122291.

Zhang, J., Lee, H.K., 2006. Application of liquid-phase microextraction and on-column derivatization combined with gas chromatography–mass spectrometry to the determination of carbamate pesticides. J. Chromatogr. A 1117, 31–37. https://doi.org/10.1016/j.chroma.2006.03.102.

Zhang, C., Schilirò, T., Gea, M., et al., 2020. Molecular basis for endocrine disruption by pesticides targeting aromatase and estrogen receptor. Int. J. Environ. Res. Public Health 17 (16), 5664. https://doi.org/10.3390/ijerph17165664.

Zhang, W., Schmull, S., Du, M., et al., 2016. Estrogen receptor α and β in mouse: adipose-derived stem cell proliferation, migration, and brown adipogenesis in vitro. Cell Physiol. Biochem. 38, 2285–2299. https://doi.org/10.1159/00044558.